EES Batteries

MINIREVIEW

View Article Online
View Journal | View Issue

Cite this: *EES Batteries*, 2025, **1**, 1102

Advancements for aqueous polysulfide-based flow batteries: development and challenge

Xinru Yang, Qingshun Nian, Yiqiao Wang, Hu Hong, Zhiquan Wei, Yue Hou and Chunyi Zhi *

Polysulfide-based redox flow batteries (PSRFBs) have emerged as an innovative solution for large-scale energy storage technology owing to their high energy density and low cost. These advantages position PSRFBs as particularly suitable for grid-scale integration of renewable energy. However, challenges such as sluggish redox kinetics and crossover of polysulfide have impeded their widespread adoption and commercialization. This review aims to provide a comprehensive overview of the working principles, development, and challenges of PSRFBs, focusing on strategies to mitigate crossover and enhance reaction kinetics of polysulfides. Recent advancements in catalytic materials, membrane design, and electrolyte engineering are summarized, highlighting their important roles in improving the electrochemical performance of PSRFBs. Future research directions for PSRFBs are finally suggested to focus on designing ion-exchange membranes with moderate ionic conductivity and ionic selectivity, developing redox mediators or soluble catalysts, tailoring the solvation structure of polysulfides in the anolyte and employing advanced *in-situ* characterization techniques.

Received 30th May 2025,
Accepted 17th July 2025

DOI: 10.1039/d5eb00107b

rsc.li/EESBatteries

Broader context

The transition to renewable energy is essential for achieving global carbon neutrality and reducing reliance on fossil fuels. However, the intermittent nature of solar and wind power necessitates the development of efficient energy storage systems to ensure grid stability. Among various electrochemical storage technologies, polysulfide-based redox flow batteries (PSRFBs) have emerged as an up-and-coming candidate due to their high energy density and low cost, offering a sustainable solution for grid-scale energy storage. Despite these advantages, broader implementation of PSRFBs faces persistent challenges, including sluggish redox kinetics and polysulfide crossover. Recent advancements in catalytic materials and membrane engineering have significantly improved the electrochemical performance of PSRFBs. Innovations such as heterojunction catalysts, soluble redox mediators, and ion-selective membranes have enhanced reaction kinetics and mitigated crossover effects, paving the way for more efficient and durable systems. The continued optimization of membrane design, the exploration of advanced catalytic materials, and the application of *in situ* characterization techniques will be critical to overcoming remaining challenges. By addressing these key issues, PSRFBs can achieve the performance and reliability required for large-scale renewable energy integration. The ongoing advancement of PSRFB technology supports their practical deployment and aligns with global efforts to build sustainable, low-carbon energy infrastructure.

1. Introduction

In recent years, energy issues have become a global focus driven by the rising requirements for advanced energy storage solutions and sustainable power conversion systems.[1,2] The transition from conventional hydrocarbon-based fossil fuels to renewable and clean energy sources, such as solar and wind power, is critical for addressing the climate issue and achieving sustainable energy security.[3] However, the inherent intermittency of these renewables presents a major barrier to their large-scale deployment, necessitating the development of reliable energy storage systems that can balance supply and demand.[4,5] Among available energy storage technologies, electrochemical energy storage stands out for its stability, scalability, and portability, making it vital for enabling large-scale renewable energy deployment.[6,7] Lithium-ion batteries were first introduced to the market in the early 1990s and have since become widely adopted for powering consumer electronics and electric vehicles, undoubtedly achieving great success.[8–10] Nevertheless, due to the limitation of lithium resources and safety concerns, the development of safe and sustainable energy storage systems remains urgent and essential.[11,12]

Aqueous redox flow batteries (RFBs) have emerged as highly promising electrochemical energy storage systems, offering inherent safety, exceptional scalability, and the unique capability for independent optimization of energy density and power

Department of Materials Science and Engineering, City University of Hong Kong, 83 Tat Chee Avenue, Kowloon, Hong Kong, 999077 P. R. China.
E-mail: cy.zhi@cityu.edu.hk

density.[13–16] In the 1970s, the first aqueous RFBs using Cr^{2+}/Cr^{3+} and Fe^{2+}/Fe^{3+} redox couples were launched by NASA.[17] RFBs using Zn/Br coupled with a phase-transition concept were also invented in the 1970s.[18] In the 1980s, all-vanadium RFBs, which have since become the most extensively developed RFB technology to date, were reported by Sum and Skyllas-Kazacos.[19,20] Up to now, tremendous achievements have been made to develop high-performance RFBs. Polysulfide-based redox species have garnered considerable attention due to their exceptional solubility (up to 8.8 mol L^{-1} in water) and low chemical cost (~US \$0.15 kWh^{-1}), and the natural abundance of sulfur, the 14th most prevalent element in the Earth's crust.[13,21–23] These advantages position polysulfide-based redox flow batteries (PSRFBs) as a highly attractive option for grid-scale energy storage, particularly in supporting renewable energy integration.[24,25]

The exploration of PSRFBs began in 1984 when R. J. Remick *et al.* introduced the first polysulfide–bromine RFB,[26] after which various configurations of PSRFBs were proposed and investigated. Fig. 1 summarizes the representative types of PSRFBs and their developmental timeline, highlighting the progression from early prototypes to advanced systems. Given the rapid advancements in polysulfide chemistry, a comprehensive review of PSRFBs is both timely and necessary. In this review, we will start by outlining the fundamental working principles and major types of PSRFBs. Subsequently, we critically review the key challenges hindering their widespread adoption, with a particular focus on strategies to minimize crossover and enhance reaction kinetics. Finally, an outlook on future research directions will be discussed, emphasizing the potential of PSRFBs to meet the growing demands of renewable energy storage.

2. Overview of polysulfide-based redox flow batteries

PSRFBs represent a promising class of electrochemical energy storage systems that leverage the unique chemistry of polysulfide species. This section will first examine the fundamental aqueous chemistry of polysulfides, focusing on their chain-length-dependent solubility, pH-dependent redox behavior, and dynamic disproportionation equilibrium. Building on these chemical principles, the development of various PSRFB configurations, including all-liquid and hybrid designs, will be overviewed.

2.1 Aqueous polysulfide chemistry

The electrochemical performance of PSRFBs is fundamentally governed by the behavior of polysulfides in aqueous electrolytes. The concentration of polysulfides in aqueous electrolytes plays a significant role in determining the volumetric capacity and energy density of PSRFBs.[27,28] While short-chain polysulfide species (S_n^{2-}, where $1 \leq n < 4$) demonstrate excellent aqueous solubility, their long-chain counterparts and elemental sulfur display either limited solubility or complete insolubility in aqueous solutons.[29,30] This solubility difference significantly impacts the electrochemical performance of PSRFBs, as it affects reaction kinetics, and the energy efficiency (EE) of the battery. Beyond solubility, the pH of the electrolyte further influences the electrochemical behavior of polysulfides. The reported Pourbaix diagram reveals that the equilibrium potential of polysulfide is pH-dependent at pH values below 11.5, but it remains stable at −0.51 V (*vs.* standard hydrogen electrode (SHE)) for pH values above 11.5.[29,31,32] The stability of polysulfides under alkaline conditions ensures consistent redox potentials and minimizes side reactions that could degrade battery performance.[31,33] In addition, polysulfides could be stabilized by the formation of HS^- through an electrolyte hydrolysis in an alkaline medium instead of generating H_2S in neutral or acidic environments.[34] This stabilization mechanism enhances the reversibility of the redox reactions in PSRFBs.[35,36] For instance, the reaction of polysulfide in water is represented as follows:

$$S_2^{2-} + 2H_2O + 2e^- \leftrightarrow 2HS^- + 2OH^-;$$
$$E^\circ = -0.51\,V\,(vs.\,SHE)$$

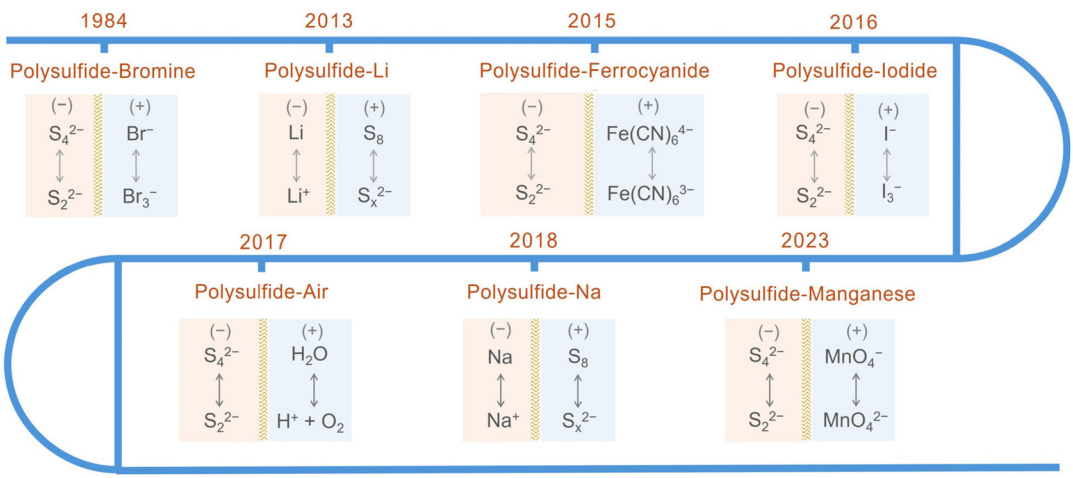

Fig. 1 A timeline of the development of representative types of PSRFBs.

The long-chain polysulfide is reduced to form short-chain polysulfide or sulfide ions accompanied by the cleavage of disulfide bonds (S–S) during the charging process. During discharge, these species reversibly convert back to their original states through the reformation of disulfide bonds.[30,31]

Polysulfides exhibit a tendency to be disproportionate in solution due to the similar Gibbs free energies of different polysulfide species, leading to dynamic equilibria between various chain lengths.[37,38] Despite this inherent instability, the key polysulfide species, such as S_2^{2-}, S_4^{2-}, and S^{2-}, have been confirmed to undergo highly reversible electrochemical reactions. This reversibility is supported by operando UV-vis spectroscopy and electrochemical studies, which provide direct evidence of the feasibility of PSRFBs for long-term energy storage (Fig. 2a). During polysulfide oxidation, the UV-vis absorption bands of S^{2-} (260 nm), S_2^{2-} (300 nm), and S_3^{2-}/S_4^{2-} (370 nm) decrease, indicating the conversion of short-chain polysulfides (S_n^{2-}, $n < 4$) to long-chain species ($4 < n < 8$).[39] Notably, long-chain polysulfides ($n \geq 4$) are insoluble and undetectable by UV-vis. Before further reduction, the absorption bands slightly increase without a reduction current, likely due to disproportionation of long-chain polysulfides into shorter chains. Upon reduction, short-chain polysulfide bands (S_n^{2-}, $n < 3$) intensify, suggesting the reduction of higher-order polysulfides (S_n^{2-}, $3 < n < 8$) to S^{2-}, S_2^{2-}, and S_3^{2-}. At the end of reduction, the S_2^{2-} band declines, reflecting further reduction to sulfides.[40] Operando electrochemical Raman spectroscopy further confirms the reversibility of polysulfide redox reactions during charging and discharging processes. The characteristic Raman peaks at 450 cm^{-1} (S_2^{2-}), 535 cm^{-1} (S_3^{2-}) and 475, 490 cm^{-1} (S_4^{2-}) are gradually reduced during the charging process. It should be noted that S^{2-} is Raman inactive, thus, it is not related to the Raman shift of S^{2-}. During the following discharge process, these spectral features exhibit complete reversibility (Fig. 2b).[41] The observed spectral reversibility directly demonstrates the robust cycling stability of this polysulfide redox couple. Among the reported PSRFBs, S_2^{2-}/S^{2-} and S_4^{2-}/S_2^{2-} redox couples are the most commonly utilized due to their favorable reaction kinetics and compatibility with aqueous electrolytes.

2.2 Development of various PSRFBs

Building on these fundamental insights, researchers have advanced the development of various PSRFB system configurations, primarily categorized into all-liquid and hybrid systems (Fig. 3). All-liquid PSRFB was invented by Remick *et al.*, coupling Na_2S_x with NaBr. This pioneering work laid the foundation for subsequent studies exploring alternative catholytes of halogen-based solutions, such as chlorine/chloride and iodine/iodide solutions.[22,40,42]

Among these halogen species, polysulfide–bromide RFBs demonstrate attractive characteristics with a high theoretical voltage of 1.35 V. However, their practical application faces significant challenges due to the hazardous nature of bromine species and the limited solubility of Br^-/Br_2 (0.21 M) in aqueous solution.[43] These limitations have driven researchers to investigate alternative iodine-based batteries, which benefit from the notably higher solubility of I^-/I_3^- in aqueous solutions.[44] The polysulfide–polyiodide flow battery (SIFB) showed a decent voltage of 1 V, maintaining stable cycling over 200 cycles (approximately 530 h, Fig. 4a).[24] SIFB represents a significant improvement in terms of safety and scalability compared to bromine-based PSRFBs. Further innovations in PSRFB design should be focused on reducing corrosivity to the equipment and improving environmental compatibility. Additionally, polysulfide species require a highly alkaline environment (typically pH > 13) to maintain stability and prevent undesirable disproportionation reactions. However, this strongly basic condition often conflicts with the optimal pH range for halogen redox couples (Br^-/Br_2 or I^-/I_3^-), which tend to exhibit better electrochemical activity in neutral or mildly acidic media. In bromine-based systems, alkaline conditions can lead to the formation of less reactive hypobromite (BrO^-), reducing battery performance.[45,46] Similarly, in polyio-

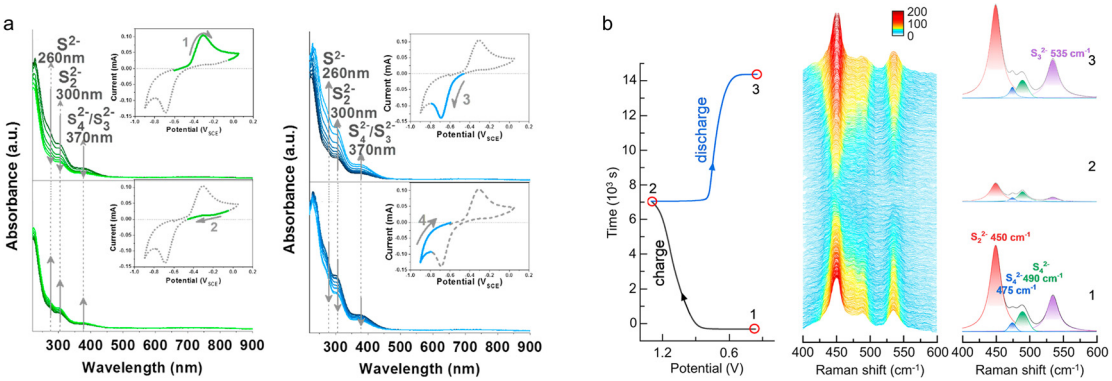

Fig. 2 (a) Operando UV-vis spectra of polysulfide redox couple during the oxidation scan (1–2) and reduction scan (3–4) of 5 mM K_2S_2 in 0.5 M KCl at 5 mV s^{-1} in the voltage range of −0.9 V_{SCE} to 0.05 V_{SCE}. Reproduced with permission.[40] Copyright 2016, Elsevier Ltd. (b) The time-resolved waterfall plot and selected Raman spectrum with the corresponding charging and discharging curves for an aqueous polysulfide electrolyte. Reproduced with permission.[41] Copyright 2023, American Chemical Society.

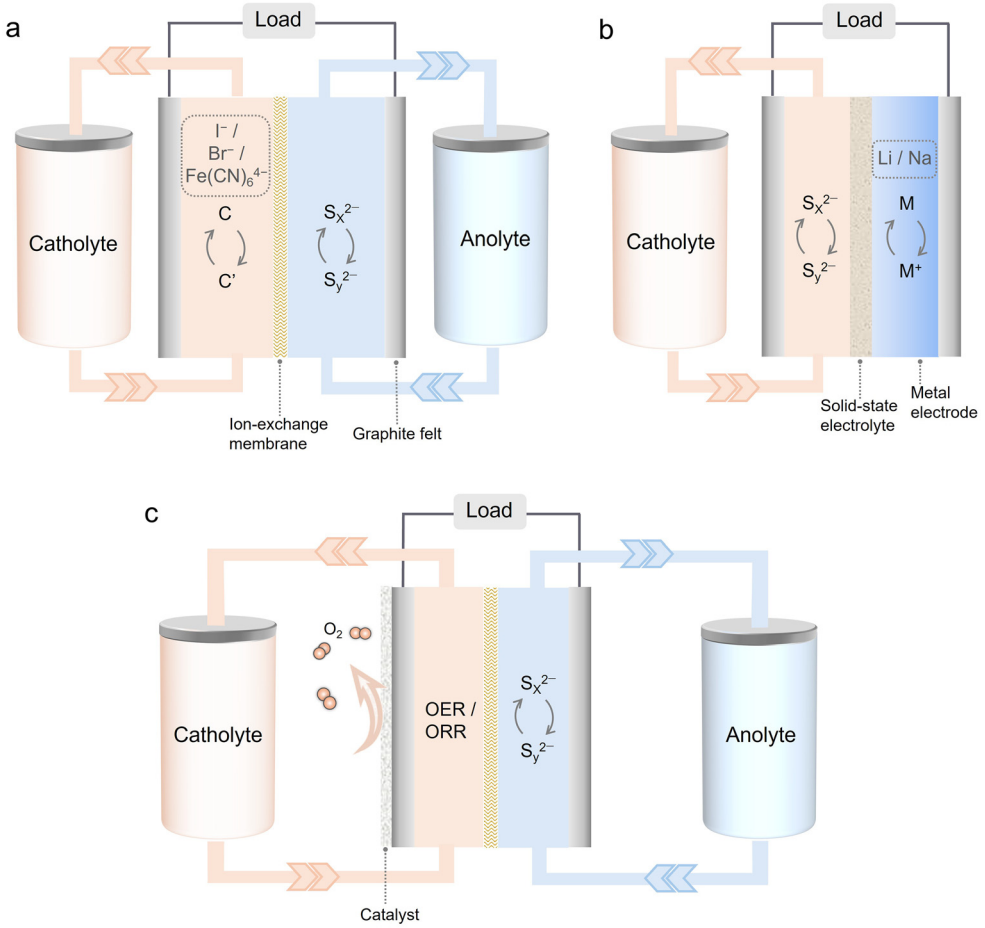

Fig. 3 Schematic illustration of architectural configurations of various PSRFBs. (a) All-liquid PSRFBs. (b) Solid–liquid PSRFBs featuring a metal electrode as the anode. (c) Liquid–gas PSRFBs employing ORR/OER reactions at the cathode current collector.

dide systems, high pH may cause iodine hydrolysis, diminishing capacity.[47] This pH mismatch necessitates careful electrolyte engineering or membrane modifications to balance the stability of polysulfides with the reactivity of halogen species, adding complexity to system design. Future research also should explore pH-buffering strategies, or alternative halogen mediators compatible with alkaline environments to address this fundamental limitation. Wei *et al.* developed novel ferri/ferrocyanide-polysulfide RFBs, exhibiting excellent electrochemical performance with a high coulombic efficiency (CE) of 99% and an EE value of 74%. Nevertheless, the energy density of this system requires further improvement due to the limited solubility (≤1.0 M) of the $[Fe(CN)_6]^{4-/3-}$ redox couple in a neutral environment.[48] Enhancing the solubility of ferri/ferrocyanide species or optimizing the electrolyte composition could further improve the energy density and overall performance of ferri/ferrocyanide-polysulfide RFBs.[49,50] Taking advantage of the counter-ion effect and the Prussian blue/Prussian white as the redox mediator (single-molecule redox-targeting reactions, SMRT), the theoretical maximum concentration of $[Fe(CN)_6]^{3-/4-}$ in the catholyte could theoretically reach up to 10.0 M at room temperature (Fig. 4b). This corresponds to an impressive theoretical volumetric capacity of 268.0 Ah L^{-1} and an energy density of 260.0 Wh L^{-1} for the $[Fe(CN)_6]^{3-/4-}$-containing catholyte. Additionally, the developed Fe/S flow battery exhibits exceptional cycling stability, demonstrating an ultralong operational lifespan exceeding 7000 cycles (4500 hours).[51] Leveraging the Earth-abundant and multivalent nature of manganese ions, the Mn^{2+}/MnO_2 redox couple was reported to pair with polysulfides. Benefiting from the low cost of both polysulfides and manganese compounds, the polysulfide–manganese RFB achieved an exceptionally low electrolyte cost of \$11.00 kWh^{-1}. Furthermore, due to the introduction of an iodide mediator to enhance MnO_2 dissolution and acetate-based electrolytes to stabilize Mn^{2+}, the battery could operate at a record-high areal capacity of 100 mAh cm^{-2}, marking a substantial advancement for Mn^{2+}/MnO_2-based energy storage technologies.[52] Unlike the Mn^{2+}/MnO_2 deposition–dissolution reaction, Ding *et al.* investigated an alternative manganese redox chemistry by employing a highly soluble MnO_4^-/MnO_4^{2-} redox couple.[53] The proposed battery showed a decent theoretical voltage of 1.068 V according to the potentials of MnO_4^-/MnO_4^{2-} (0.558 V *vs.* Hg/HgO) and S_4^{2-}/S_2^{2-} (−0.510 V *vs.* Hg/HgO) redox pairs (Fig. 4c). The energy density of this cell is

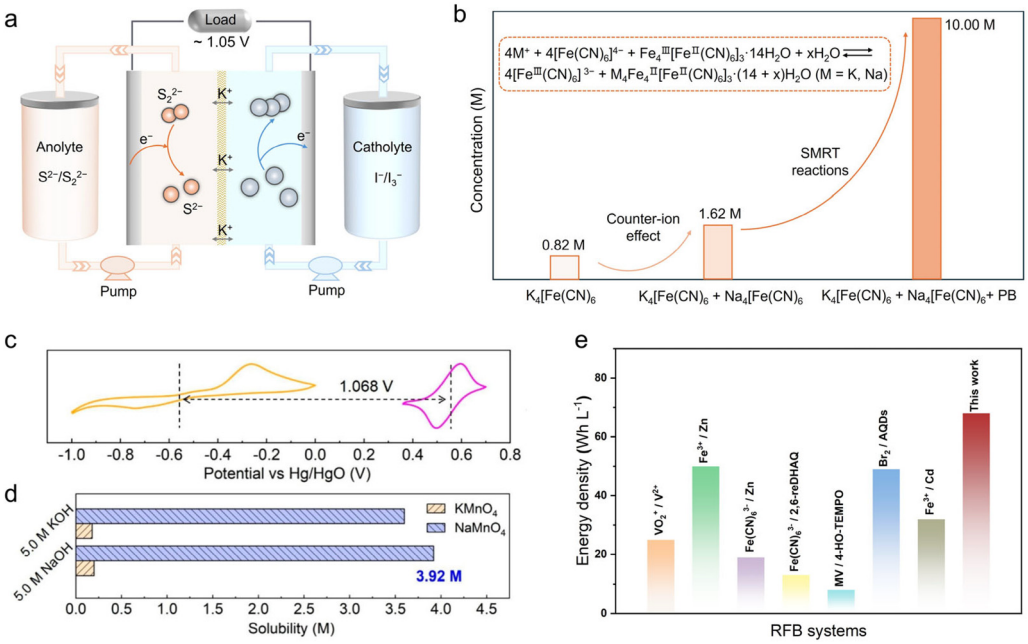

Fig. 4 (a) A schematic illustration of the proposed SIFB. (b) Calculation of the theoretical concentration of $[Fe(CN)_6]^{4-}$ with different strategies when the catholyte is the capacity-limiting side. (c) Cyclic voltammetry (CV) curves of 50 mM $NaMnO_4$ in 5.0 M NaOH solution and 50 mM Na_2S_2 in 5.0 M NaOH solution, respectively. Reproduced with permission.[53] Copyright 2023, American Chemical Society. (d) Comparisons of solubility limits of $NaMnO_4$ and $KMnO_4$ in different alkaline-supporting electrolytes under ambient temperature. Reproduced with permission.[53] Copyright 2023, American Chemical Society. (e) Comparisons of the energy density between the proposed S/Mn RFB and some representative reported RFB systems.[55–61]

constrained by the catholyte concentration, primarily due to the significantly lower solubility of $KMnO_4$ (0.2 M) compared to $NaMnO_4$ (3.92 M) in alkaline media (Fig. 4d). This innovative design enabled a polysulfide/permanganate RFB to achieve a remarkable energy density of 67.8 Wh L^{-1} with low chemical costs ($17.31 kWh^{-1}), making it particularly attractive for cost-effective grid-scale storage (Fig. 4e). However, the practical deployment of the RFB faces challenges stemming from the strong oxidative and corrosive nature of the MnO_4^-/MnO_4^{2-} redox couple, which could degrade battery components (*e.g.*, membranes, electrodes) and compromise long-term stability.[54] A comprehensive performance comparison of these PSRFB technologies can be found in Table 1.

The development of lithium/sodium-polysulfide RFBs has emerged as an attractive approach for large-scale energy storage, leveraging the high theoretical energy density of alkali metal anodes combined with the flowable aqueous polysulfide catholyte.[62–65] However, a major challenge arises from the intrinsic incompatibility between aqueous electrolytes and lithium metal, as the highly reactive lithium anode can readily react with water, leading to safety concerns and battery failure. Researchers have implemented solid electrolyte separators such as lithium superionic conductor (LISICON) separators to overcome this critical limitation, which effectively isolates the metallic lithium anode from the aqueous catholyte.[66] Based on the Li_2S_4/Li_2S redox couple with high solubility (over 5.0 M in H_2O), aqueous lithium–polysulfide batteries achieve a high density of 387 Wh L^{-1}.[29,67] This makes them highly competitive for energy storage applications requiring high capacity and efficiency. Unfortunately, the dendrite formation of lithium metal usually results in battery failure during long-term cycles, which still remains a challenge.[68]

Table 1 Summary of PSRFBs based on all-liquid configuration

Electrolyte composition	E_{cell} (V)	J (mA cm^{-2})	Membrane	Cycle life
3.3 M K_2S_2–1 M KOH || 6 M KI	1.05	5–25	N117	50 cycles (ref. 40)
1.3 M Na_2S_4–1 M NaOH || 4 M NaBr	1.35	40	N117	50 cycles (ref. 43)
1 M Na_2S_2 || 1 M $K_3Fe(CN)_6$	0.91	20–50	N117	100 cycles (ref. 48)
2.0 M K_2S–1.0 M KCl || 0.65 M $K_4[Fe(CN)_6]$–0.65 M $Na_4[Fe(CN)_6]$–0.5 M KCl–10.4 mM PB granules	0.86	20–120	N212	200 cycles per 480 h (ref. 51)
2 M K_2S_2–1 M KOH || 1.5 M $Mn(Ac)_2$–2 M KAc–1.5 M KCl–0.2 M KI	1.20	10	N117 with a Ketjen black carbon layer	75 cycles per 500 h (ref. 52)
2 M Na_2S_2–5 M NaOH || 1 M $NaMnO_4$–5 M NaOH	1.20	20	N212	100 cycles per 220 h (ref. 53)

Inspired by the oxygen reduction reaction (ORR) and the oxygen evolution reaction (OER), researchers have developed an innovative air-breathing PSRFB. This hybrid architecture couples a polysulfide anolyte with an oxygenated or aerated catholyte, employing a solid-state LiSICON-type electrolyte separator to prevent cross-contamination between redox-active solutions.[21] Through this approach, the hybrid PSRFBs could achieve an energy density ranging from 30 to 145 Wh L^{-1} by controlling the concentration of polysulfides in the catholyte. Exploiting sulfur's intrinsic advantages, the chemical cost of the active materials in the full battery was estimated to be as low as approximately $1 per kWh of stored energy, making it an economically attractive option for large-scale energy storage.[69] Despite these advantages, the air-breathing PSRFB faces several challenges that limit its performance. Specifically, the limited ionic conductivity of the solid-state electrolyte restricts ion transport, while the sluggish redox kinetics of both the polysulfide anolyte and the oxygen-based catholyte reduce the overall power density of the system.[70,71] Additionally, the reliance on noble-metal catalysts, such as platinum or iridium, to facilitate the ORR and OER in the liquid–gas hybrid system significantly increases the overall cost of the battery.[72]

3. The common challenges of PSRFBs

PSRFBs have shown up-and-coming prospects for energy storage applications. However, some critical challenges still exist, including poor kinetics of polysulfides, especially during the electrochemical reduction process, and the severe cross-over of polysulfides, leading to capacity decay and voltage efficiency loss. In the following, we will introduce these issues and the corresponding strategies for the development of PSRFB applications. Overcoming these limitations is the key to advancing PSRFBs toward commercialization.

3.1 Poor kinetics of polysulfide for the electrochemical redox process

One of the most pressing challenges in aqueous PSRFBs is the sluggish reaction kinetics, especially during the polysulfide reduction process. This kinetic limitation manifests as severe polarization, with overpotentials exceeding 500 mV even at a low current density of 10 mA cm^{-2}, leading to a low EE and power density.[73,74] Therefore, it is necessary to catalyze and facilitate the charge transfer process of polysulfide and improve the overall performance of PSRFBs. Ge *et al.* first used a Ni/C catalyst to improve the performance of polysulfide.[75] A cell potential efficiency of up to 88.2% was obtained at 0.1 A cm^{-2}. Building on this, Zhao *et al.* employed nickel foam as the electrocatalytic negative electrode to catalyze the kinetic performance of S_4^{2-} in PSRFBs.[43] Due to the formation of Ni/NiS_x, which are suitable catalytic materials on the surface of the electrode, the overall EE of the PSRFB could average up to 77.2% at 40 mA cm^{-2}, and the power density is about 56 mW cm^{-2}. These findings demonstrated the potential of nickel-based catalysts in improving the kinetic performance of PSRFBs. After that, various metal sulfides, including CuS, CoS and WS_2, and metal sulfide–carbon nanotube composites have been applied as catalysts to enhance the kinetic properties of polysulfide. CuS was proved to demonstrate stable catalytic performance for polysulfide–air batteries.[76] Gao *et al.* further coated CuS on graphite felt (GF) by a successive ionic layer adsorption and reaction (SILAR) technique. The strong anchoring effect between CuS and polysulfides enabled a higher local polysulfide concentration on the GF surface, thereby enhancing reaction kinetics. When paired with the $[Fe(CN)_6]^{4-/3-}$ catholyte, the resulting RFB delivered a high peak power density of 116 mW cm^{-2} at 220 mA cm^{-2} and maintained an EE of 77.7% at 50 mA cm^{-2}.[77] Cobalt sulfide has multiple chemical formulas and can form heterojunctions with itself. Such a built-in field of heterojunction can accelerate the transport of charge carriers.[78,79] Hence, a CoS_2/CoS n–n heterojunction-modified GF was employed to electrochemically catalyze the redox reaction of polysulfide (Fig. 5a and b). The PSRFB exhibited a peak power of 86.2 mW cm^{-2}, while maintaining 96% EE retention throughout 1000 hours of continuous cycling, which is attributed to the uneven charge distribution of the CoS_2/CoS heterojunction and thereby the improved absorptivity of charged ions (Fig. 5c).[80] To further improve the intrinsic activity of MoS_2, the Co single atom anchoring onto the MoS_2 (Co_{SA}-V_S/MoS_2) surface has been explored to introduce highly active catalytic sites, and optimize the comprehensive performance of PSRFBs (Fig. 5d). The incorporation of Co single atoms induced sulfur vacancies and a phase transition from semiconducting 2H to metallic 1T-MoS_2, significantly improving charge transfer and redox kinetics. The derived PSRFB delivered a peak power density of 95.7 mW cm^{-2}, among the highest reported for PSRFBs (Fig. 5e). Moreover, the battery maintained a high EE value of 76.5% at 30 mA cm^{-2} over 50 cycles, demonstrating the stability of Co_{SA}-V_S/MoS_2.[81] Fan *et al.* systematically compared MoS_2, WS_2, and Cu-doped MoS_2 as film electrodes for polysulfide reactions. The authors found that the catalytic activity of these film electrodes was initially high, while the Cu-doped MoS_2 catalyst exhibited robust stability over the cycling process.[82] Sulfide-based catalysts like CuS, CoS, and MoS_2 exhibit excellent catalytic activity for polysulfide redox reactions due to their strong sulfur affinity. This intrinsic property enables effective chemisorption of polysulfide intermediates through metal–sulfur bonding, which facilitates electron transfer and stabilizes reaction intermediates. The sulfur-rich surfaces provide abundant active sites that lower the energy barrier for polysulfide conversion reactions, significantly improving the reaction kinetics. Chen *et al.* also applied a CoZn–N–C membrane electrode to facilitate the redox kinetics of polysulfide. DFT calculations revealed that the stronger adsorption interactions and a larger amount of electron transfer between S_2^{2-} and Co–N_4 could effectively weaken the S–S bond and thus reduce the decomposition barriers of S_2^{2-} (Fig. 5f). Cyclic voltammetry analysis revealed significantly improved redox kinetics for polysulfides when using

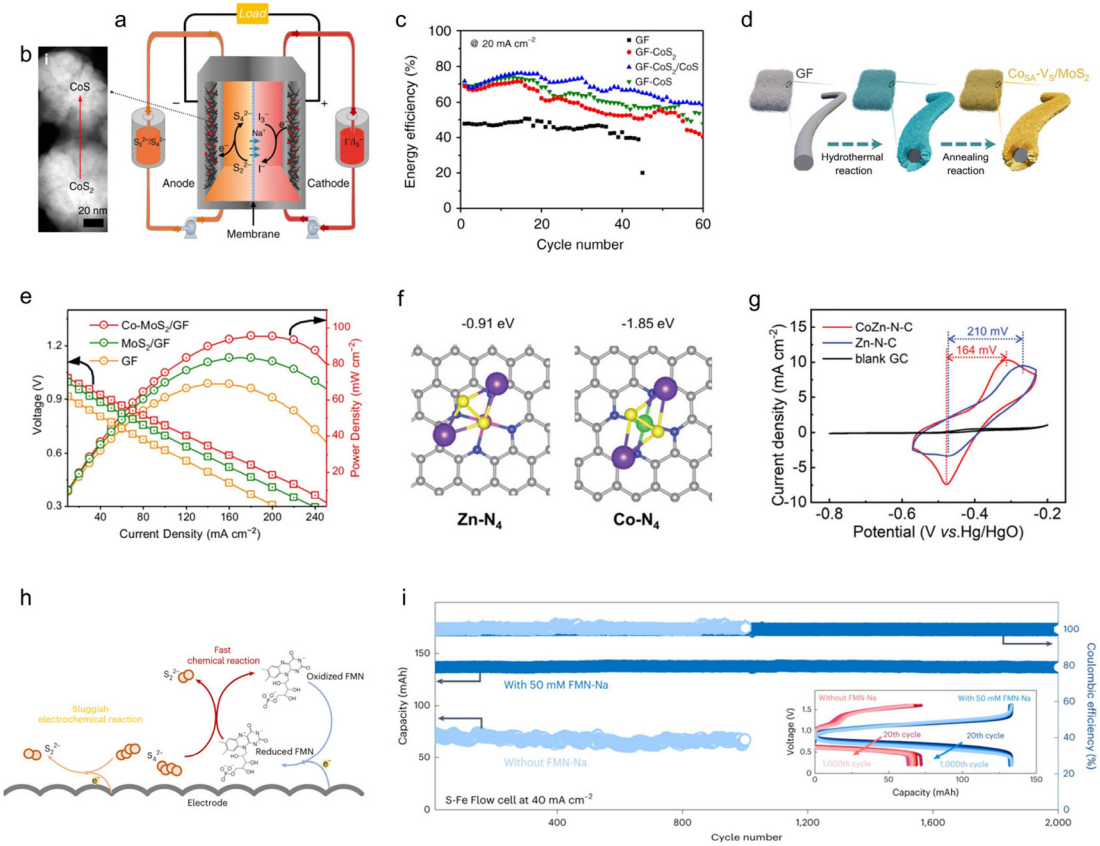

Fig. 5 (a) Schematic of the SIFB configuration. (b) High-angle annular dark-field scanning transmission electron microscopic image of CoS_2/CoS with an arrow indicating the direction of the electron energy loss spectral line scan. (c) The EE of the SIFBs at 20 mA cm^{-2}. Reproduced with permission.[80] Copyright 2019, The Authors, Springer Nature. (d) Schematic of the Co_{SA}-V_S/MoS_2 synthetic process. (e) Discharge curves and the corresponding power densities of SIFBs with 50% state of charge. Reproduced with permission.[81] Copyright 2025, The Authors, Springer Nature. (f) Calculated stable geometric configurations of Na_2S_2 and Zn–N_4 (left panel), Na_2S_2 and Co–N_4 (right panel). Color codes: purple (Na), yellow (S), blue (N), gray (C), pink (Zn), and green (Co). (g) CV curves of 0.1 M Na_2S_2. Reproduced with permission.[83] Copyright 2023, Wiley-VCH GmbH. (h) Proposed reaction pathway of molecular-catalyst sodium riboflavin phosphates (FMN-Na) to accelerate polysulfide and the traditional reduction pathway of polysulfide. (i) Cycling performance of the S–Fe RFBs with (dark blue) or without (light blue) FMN-Na at 40 mA cm^{-2}. The inset shows the voltage profiles of S–Fe RFBs from the 20th to 1000th cycle. Reproduced with permission.[84] Copyright 2023, Springer Nature.

the CoZn–N–C electrocatalyst, demonstrating a remarkably low overpotential of only 164 mV. In contrast, the pristine GF substrate showed negligible electrochemical activity under the same scan conditions, with no discernible oxidation or reduction peaks observed (Fig. 5g). The PSRFB achieved a high EE of 88.4% at 10 mA cm^{-2} and a remarkably low capacity fade rate of 0.0025% per cycle during 200 cycles at 60 mA cm^{-2}.[83] The nanoconfined self-assembled ordered hierarchical porous Co and N codoped carbon (OHP-Co/NC) was applied as an electrocatalytic catalyst to promote polysulfide mass transfer. When implemented in a membrane–electrode assembly configuration, the OHP-Co/NC-850 catalyst enabled the PSRFB to achieve an exceptional power density of 110 mW cm^{-2}.[41]

Different from the reported solid catalysts, Lei *et al.* developed a homogeneous catalytic system employing riboflavin sodium phosphate (FMN-Na) as a redox mediator for polysulfide conversion. This innovative approach effectively transformed the inherently sluggish polysulfide redox reactions into rapid FMN-Na-mediated electron transfer processes (Fig. 5h). The resulting ferri/ferrocyanide-polysulfide redox flow battery exhibited exceptional cycling stability, maintaining performance over 2000 cycles at 40 mA cm^{-2} with an ultralow capacity decay rate of merely 0.00004% per cycle (equivalent to 0.0017% per day) (Fig. 5i).[84] These advancements highlight the potential of catalytic strategies to address the kinetic limitations of PSRFBs. Future design should develop more efficient, cost-effective and sustainable catalysts, ultimately advancing the scale-up performance of PSRFBs.

3.2 Crossover of polysulfide active species

Server crossover of polysulfide poses a significant challenge, hindering further scale-up and practical application of PSRFBs. The crossover of polysulfide not only accelerates water migration but also increases the redox overpotential, as polysulfide will be oxidized by the catholyte and generate insulating precipitates on the electrode. Furthermore, these insulating sulfur precipitates may also deposit within the membrane pores, which significantly increases ionic resistance and accel-

erates membrane degradation through physical blockage and localized stress.[85] To address this challenge, researchers have explored various membrane-based solutions. Li *et al.* used two layers of membranes, N117 and N115, to inhibit the crossover of polysulfide. The PSRFB showed high-capacity retention (>98%) with high CE (>97%) over 50 cycles under the state of charge (SOC) of 80%. While this strategy improved the CE of the battery, it simultaneously compromised the voltage efficiency (VE), further limiting the poor kinetics of the polysulfide.[40] Similarly, Xia *et al.* also employed a modular dual-membrane architecture by combining an anion-exchange membrane (AEM, FAA-3-PK-130) and a cation-exchange membrane (CEM, N117). The dual membranes could effectively mitigate the crossover of polysulfide and offer moderate conductivity of OH^- (Fig. 6a). The polysulfide–air RFB showed an average round-trip EE value of 40% at 1 mA cm^{-2} over 80 cycles.[86] In addition to membrane-based solutions, solid-state electrolytes (SSEs) have been investigated as an alternative to traditional Nafion separators. Gross *et al.* implemented solid-state electrolytes, including NASICON ($Na_3Zr_2Si_2PO_{12}$) and LATP ($Li_{1+x+y}Al_xTi_{2-x}P_{3-y}Si_yO_{12}$) as ionic conductors to effectively mitigate polysulfide crossover. The polysulfide–polybromide battery operated over 1600 h at 0.5 mA cm^{-2} under 50% SOC. However, the low ionic conductivity for LATP (~1.0×10^{-4} S cm^{-1}) and for NASICON (~1.0×10^{-3} S cm^{-1}) hindered the EE and power density of batteries with low operating current densities. Additionally, the instability of NASICON ceramics in highly corrosive polyhalide catholytes would result in capacity decay, highlighting the need for more robust materials.[87] Limited by the low ionic selectivity and high cost of Nafion membrane, Sreenath *et al.* developed a cost-effective membrane based on poly(vinylidene fluoride-*co*-hexafluoropropylene) (PVDF-*co*-HFP). The membrane effectively suppressed polysulfide crossover through thermal densification treatment while maintaining excellent ionic conductivity *via* controlled sulfonation (Fig. 6b). The PSRFB exhibited a high CE of 99.4% and a moderate EE of 63.0% over 250 cycles at 40 mA cm^{-2}.[88] Li *et al.* designed a charge-reinforced ion-selective (CRIS) membrane by coating carbon onto a Nafion membrane to effectively adsorb polysulfide anions on the negative current collector (Fig. 6c). The CRIS membrane exhibited significantly reduced polychalcogenide permeability while maintaining ionic resistance comparable to that of double N117/N115 membranes. Furthermore, the incorporation of PVDF enhanced the membrane's hydrophobicity, effectively suppressing OH^- migration. When applied in the SIFB with 4.0 M KI as the catholyte and 2.0 M K_2S_2 as the anolyte, the membrane enabled a stable cycling performance over 500 cycles, equivalent to 3.1 months of continuous operation (Fig. 6d).[85] Mitigating the crossover of polysulfide is critical for advancing PSRFBs toward large-scale energy storage applications. It is important to maintain the power density of PSRFBs when designing membranes to improve the cycling stability of polysulfide.

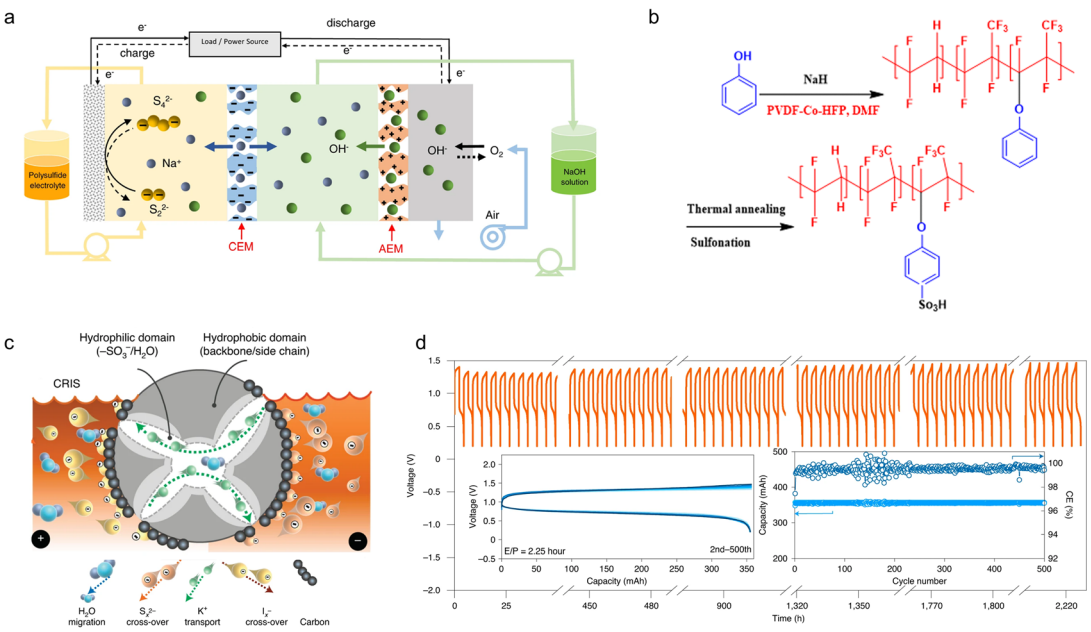

Fig. 6 (a) Polysulfide–air RFB employing a dual-membrane design combining an AEM and a CEM. Reproduced with permission.[86] Copyright 2022, The Authors, Springer Nature. (b) Reaction scheme for the synthesis of phenol-docked PVDF-*co*-HFP polymer and subsequent thermal annealing to produce a CEM. Reproduced with permission.[88] Copyright 2024, Royal Society of Chemistry. (c) Schematic of the CRIS membrane, of which the negatively charged carbon layer mitigates the crossover of the negatively charged active species (S_x^{2-} and I_x^-), and the hydrophobic PVDF alleviates water migration at the same time. (d) Voltage profiles of SIFB at 10 mA cm^{-2} with an energy-to-power ratio (E/P) of 2.25 h. The insets show the representative voltage profiles from the 2nd to 500th cycle, CE and capacity retention over 500 cycles (catholyte: 10.0 ml 4.0 M KI, anolyte: 10.0 ml 2.0 M K_2S_2–1.0 M KOH, 16 cm^2 membrane area). Reproduced with permission.[85] Copyright 2021, Springer Nature.

4. Summary and outlook

As an energy storage technology that fulfills the critical requirements of safety and cost-effectiveness for large-scale applications, PSRFBs have attracted significant attention due to their high energy density, low cost, and scalability. Despite their great potential, PSRFBs still face challenges such as sluggish redox kinetics, crossover of polysulfide, and the need for stable and cost-effective components (including catalysts and ion-exchange membranes). Significant progress has been made in recent years to address these issues. Although some existing methods have successfully achieved high-performance PSRFBs, it should be recognized that there is still a long way to go before the widespread commercialization of PSRFBs. For the future development of PSRFBs, we believe the following aspects should be prioritized (Fig. 7).

(1) Designing ion-exchange membranes to balance ionic conductivity and ionic selectivity. An ideal membrane of PSRFBs should simultaneously combine high ionic conductivity for charge carrier transport with effective suppression of the cross-over of polysulfide, thereby maintaining the high power density and long lifespan of PSRFBs. Moreover, membrane design must also consider cost-effectiveness to facilitate large-scale deployment.

(2) Developing redox mediators or soluble catalysts. Compared to solid catalysts attached to GF, the incorporation of liquid catalysts offers a more straightforward approach while leveraging the inherent advantages of the flow nature. These soluble species can significantly enhance the reaction kinetics of multi-electron transfer processes in PSRFBs. Furthermore, redox mediators enable higher energy density through optimized cell configurations. Notably, a key challenge lies in mitigating the self-discharge effect of organic redox mediators, which can lead to capacity loss and must be carefully addressed in material selection and battery design.

(3) Tailoring the solvation structure of polysulfides in the anolyte. Although the crossover is influenced by the osmotic pressure of the active species, regulating the interaction between polysulfides and the electrolyte can help reduce the formation of insulating precipitates, mitigate crossover, and enhance overall battery performance, which is rarely reported for PSRFBs.

(4) Employing advanced characterization techniques. The adoption of more characterization methods, particularly *in situ* techniques, is crucial for gaining deeper insights into the reaction mechanisms and degradation processes in PSRFBs. Currently, *in situ* UV-vis and Raman spectroscopy techniques have been utilized to investigate the bulk phase transformations of polysulfide electrolytes. In the future, it may be better to design *in situ* characterization tools specifically for probing electrode surfaces, enabling real-time monitoring of charge transfer processes during electrochemical redox reactions.

In conclusion, PSRFBs represent a highly promising technology for large-scale energy storage, offering an optimal combination of high energy density, cost-effectiveness, and sustainability. By addressing these challenges in developing advanced membranes and catalysts, PSRFBs will play an increasingly pivotal role in renewable energy integration, industrial-scale energy management, and broader commercial applications.

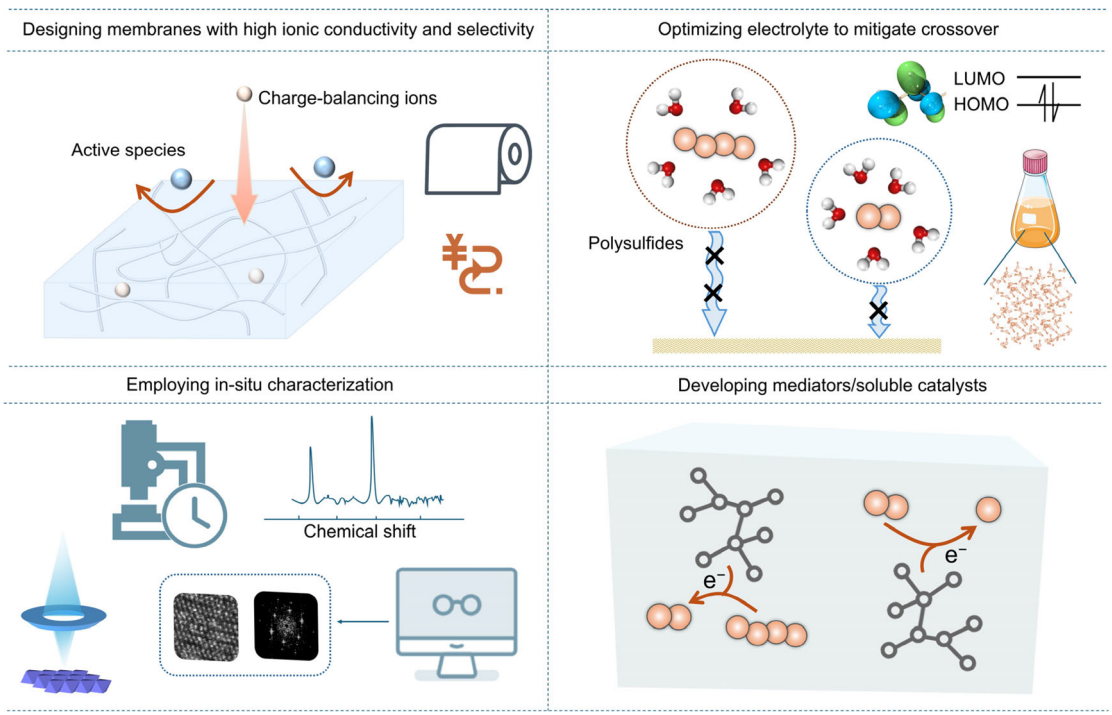

Fig. 7 A summary of key solutions to boost high-performance PSRFBs.

Conflicts of interest

The authors declare no conflict of interest.

Data availability

This review does not include any primary research results, software, or code, nor does it involve the generation or analysis of new data.

Acknowledgements

The work described in this paper was supported by a grant from the Research Grants Council of the Hong Kong Special Administrative Region, China (Project No. R1004-24F).

References

1 D. Larcher and J. M. Tarascon, Towards greener and more sustainable batteries for electrical energy storage, *Nat. Chem.*, 2015, **7**(1), 19–29.
2 Y.-h. Zhu, Y.-f. Cui, Z.-l. Xie, Z.-b. Zhuang, G. Huang and X.-b. Zhang, Decoupled aqueous batteries using pH-decoupling electrolytes, *Nat. Rev. Chem.*, 2022, **6**(7), 505–517.
3 D. Chao, W. Zhou, F. Xie, C. Ye, H. Li, M. Jaroniec and S.-Z. Qiao, Roadmap for advanced aqueous batteries: From design of materials to applications, *Sci. Adv.*, 2020, **6**(21), eaba4098.
4 L. Jiang, D. Dong and Y.-C. Lu, Design strategies for low temperature aqueous electrolytes, *Nano Res. Energy*, 2022, **1**, 9120003.
5 Z. Chen and C. Zhi, Chalcogens for high-energy batteries, *Nat. Rev. Mater.*, 2025, **10**(4), 268–284.
6 N. Kittner, F. Lill and D. M. Kammen, Energy storage deployment and innovation for the clean energy transition, *Nat. Energy*, 2017, **2**(9), 17125.
7 B. Dunn, H. Kamath and J.-M. Tarascon, Electrical energy storage for the grid: A battery of choices, *Science*, 2011, **334**(6058), 928–935.
8 M. Armand and J. M. Tarascon, Building better batteries, *Nature*, 2008, **451**(7179), 652–657.
9 J.-L. Brédas, J. M. Buriak, F. Caruso, K.-S. Choi, B. A. Korgel, M. R. Palacín, K. Persson, E. Reichmanis, F. Schüth, R. Seshadri and M. D. Ward, An electrifying choice for the 2019 Chemistry Nobel Prize: Goodenough, Whittingham, and Yoshino, *Chem. Mater.*, 2019, **31**(21), 8577–8581.
10 Y. Guo, S. Wu, Y.-B. He, F. Kang, L. Chen, H. Li and Q.-H. Yang, Solid-state lithium batteries: Safety and prospects, *eScience*, 2022, **2**(2), 138–163.
11 M. S. Whittingham, Ultimate limits to intercalation reactions for lithium batteries, *Chem. Rev.*, 2014, **114**(23), 11414–11443.
12 C. Vaalma, D. Buchholz, M. Weil and S. Passerini, A cost and resource analysis of sodium-ion batteries, *Nat. Rev. Mater.*, 2018, **3**(4), 18013.
13 G. L. Soloveichik, Flow batteries: Current status and trends, *Chem. Rev.*, 2015, **115**(20), 11533–11558.
14 M. Gao, Z. Wang, D. G. Lek and Q. Wang, Towards high power density aqueous redox flow batteries, *Nano Res. Energy*, 2023, **2**, e9120045.
15 Z. Zhao, X. Liu, M. Zhang, L. Zhang, C. Zhang, X. Li and G. Yu, Development of flow battery technologies using the principles of sustainable chemistry, *Chem. Soc. Rev.*, 2023, **52**(17), 6031–6074.
16 M. L. Lehmann, L. Tyler, E. C. Self, G. Yang, J. Nanda and T. Saito, Membrane design for non-aqueous redox flow batteries: Current status and path forward, *Chem*, 2022, **8**(6), 1611–1636.
17 L. H. Thaller, Electrically rechargeable REDOX flow cell, *US Patent* 19770007638, 1976.
18 H. S. Lim, A. M. Lackner and R. C. Knechtli, Zinc–bromine secondary battery, *J. Electrochem. Soc.*, 1977, **124**(8), 1154.
19 E. Sum and M. Skyllas-Kazacos, A study of the V(II)/V(III) redox couple for redox flow cell applications, *J. Power Sources*, 1985, **15**(2), 179–190.
20 M. Skyllas-Kazacos, M. Rychick and R. Robins, All-vanadium redox battery, *US Patent* 786567, 1988, 4.
21 Z. Li, M. S. Pan, L. Su, P.-C. Tsai, A. F. Badel, J. M. Valle, S. L. Eiler, K. Xiang, F. R. Brushett and Y.-M. Chiang, Air-breathing aqueous sulfur flow battery for ultralow-cost long-duration electrical storage, *Joule*, 2017, **1**(2), 306–327.
22 S. Zhang, W. Guo, F. Yang, P. Zheng, R. Qiao and Z. Li, Recent progress in polysulfide redox-flow batteries, *Batteries Supercaps*, 2019, **2**(7), 627–637.
23 B. Mason, *Principles of geochemistry*, LWW, 1952, vol. 74.
24 L. Su, A. F. Badel, C. Cao, J. J. Hinricher and F. R. Brushett, Toward an inexpensive aqueous polysulfide–polyiodide redox flow battery, *Ind. Eng. Chem. Res.*, 2017, **56**(35), 9783–9792.
25 F. Zhu, W. Guo and Y. Fu, Functional materials for aqueous redox flow batteries: Merits and applications, *Chem. Soc. Rev.*, 2023, **52**(23), 8410–8446.
26 R. J. Remick and P. G. Ang, Electrically rechargeable anionically active reduction–oxidation electrical storage-supply system, *US Patent* 4485154A, 1984, 27.
27 Y. Yao, J. Lei, Y. Shi, F. Ai and Y.-C. Lu, Assessment methods and performance metrics for redox flow batteries, *Nat. Energy*, 2021, **6**(6), 582–588.
28 H. Fan, K. Liu, X. Zhang, Y. Di, P. Liu, J. Li, B. Hu, H. Li, M. Ravivarma and J. Song, Spatial structure regulation towards armor-clad five-membered pyrroline nitroxides catholyte for long-life aqueous organic redox flow batteries, *eScience*, 2024, **4**(1), 100202.
29 N. Li, Z. Weng, Y. Wang, F. Li, H.-M. Cheng and H. Zhou, An aqueous dissolved polysulfide cathode for lithium–sulfur batteries, *Energy Environ. Sci.*, 2014, **7**(10), 3307–3312.

30 Z. Li and Y.-C. Lu, Material design of aqueous redox flow batteries: Fundamental challenges and mitigation strategies, *Adv. Mater.*, 2020, **32**(47), 2002132.
31 R. Demir-Cakan, M. Morcrette, J.-B. Leriche and J.-M. Tarascon, An aqueous electrolyte rechargeable Li-ion/polysulfide battery, *J. Mater. Chem. A*, 2014, **2**(24), 9025–9029.
32 R. Demir-Cakan, M. Morcrette and J.-M. Tarascon, Use of ion-selective polymer membranes for an aqueous electrolyte rechargeable Li-ion–polysulphide battery, *J. Mater. Chem. A*, 2015, **3**(6), 2869–2875.
33 C. G. Anderson, Alkaline sulfide gold leaching kinetics, *Miner. Eng.*, 2016, **92**, 248–256.
34 D. Peramunage and S. Licht, A Solid Sulfur Cathode for Aqueous Batteries, *Science*, 1993, **261**(5124), 1029–1032.
35 C. Yang, L. Suo, O. Borodin, F. Wang, W. Sun, T. Gao, X. Fan, S. Hou, Z. Ma, K. Amine, K. Xu and C. Wang, Unique aqueous Li-ion/sulfur chemistry with high energy density and reversibility, *Proc. Natl. Acad. Sci. U. S. A.*, 2017, **114**(24), 6197–6202.
36 S. Licht and D. Peramunage, Novel aqueous aluminum/sulfur batteries, *J. Electrochem. Soc.*, 1993, **140**(1), L4.
37 S. S. Zhang, Liquid electrolyte lithium/sulfur battery: Fundamental chemistry, problems, and solutions, *J. Power Sources*, 2013, **231**, 153–162.
38 Q. Zou and Y.-C. Lu, Solvent-dictated lithium sulfur redox reactions: An operando UV–vis spectroscopic study, *J. Phys. Chem. Lett.*, 2016, **7**(8), 1518–1525.
39 N. Li, Y. Wang, D. Tang and H. Zhou, Integrating a photocatalyst into a hybrid lithium–sulfur battery for direct storage of solar energy, *Angew. Chem., Int. Ed.*, 2015, **54**(32), 9271–9274.
40 Z. Li, G. Weng, Q. Zou, G. Cong and Y.-C. Lu, A high-energy and low-cost polysulfide/iodide redox flow battery, *Nano Energy*, 2016, **30**, 283–292.
41 J. Lan, K. Li, L. Yang, Q. Lin, J. Duan, S. Zhang, X. Wang and J. Chen, Hierarchical nano-electrocatalytic reactor for high performance polysulfides redox flow batteries, *ACS Nano*, 2023, **17**(20), 20492–20501.
42 C. Ponce de León, A. Frías-Ferrer, J. González-García, D. A. Szánto and F. C. Walsh, Redox flow cells for energy conversion, *J. Power Sources*, 2006, **160**(1), 716–732.
43 P. Zhao, H. Zhang, H. Zhou and B. Yi, Nickel foam and carbon felt applications for sodium polysulfide/bromine redox flow battery electrodes, *Electrochim. Acta*, 2005, **51**(6), 1091–1098.
44 C. Xie, H. Zhang, W. Xu, W. Wang and X. Li, A long cycle life, self-healing zinc–iodine flow battery with high power density, *Angew. Chem., Int. Ed.*, 2018, **57**(35), 11171–11176.
45 Y. Zhao, Y. Ding, J. Song, L. Peng, J. B. Goodenough and G. Yu, A reversible Br_2/Br^- redox couple in the aqueous phase as a high-performance catholyte for alkali-ion batteries, *Energy Environ. Sci.*, 2014, **7**(6), 1990–1995.
46 Y. Zhao, L. Wang and H. R. Byon, High-performance rechargeable lithium-iodine batteries using triiodide/iodide redox couples in an aqueous cathode, *Nat. Commun.*, 2013, **4**(1), 1896.
47 C. Xu, C. Lei, P. Jiang, W. Yang, W. Ma, X. He and X. Liang, Practical high-energy aqueous zinc–bromine static batteries enabled by synergistic exclusion-complexation chemistry, *Joule*, 2024, **8**(2), 461–481.
48 X. Wei, G.-G. Xia, B. Kirby, E. Thomsen, B. Li, Z. Nie, G. G. Graff, J. Liu, V. Sprenkle and W. Wang, An aqueous redox flow battery based on neutral alkali metal ferri/ferrocyanide and polysulfide electrolytes, *J. Electrochem. Soc.*, 2016, **163**(1), A5150.
49 H. Zou, Z. Xu, L. Xiong, J. Wang, H. Fu, J. Cao, M. Ding, X. Wang and C. Jia, An alkaline S/Fe redox flow battery endowed with high volumetric-capacity and long cycle-life, *J. Power Sources*, 2024, **591**, 233856.
50 Y. Chen, M. Zhou, Y. Xia, X. Wang, Y. Liu, Y. Yao, H. Zhang, Y. Li, S. Lu, W. Qin, X. Wu and Q. Wang, A stable and high-capacity redox targeting-based electrolyte for aqueous flow batteries, *Joule*, 2019, **3**(9), 2255–2267.
51 S. Yan, S. Huang, H. Xu, L. Li, H. Zou, M. Ding, C. Jia and Q. Wang, Redox targeting-based neutral aqueous flow battery with high energy density and low cost, *ChemSusChem*, 2023, **16**(19), e202300710.
52 J. Lei, Y. Yao, Y. Huang and Y.-C. Lu, A highly reversible low-cost aqueous sulfur–manganese redox flow battery, *ACS Energy Lett.*, 2023, **8**(1), 429–435.
53 M. Ding, H. Fu, X. Lou, M. He, B. Chen, Z. Han, S. Chu, B. Lu, G. Zhou and C. Jia, A stable and energy-dense polysulfide/permanganate flow battery, *ACS Nano*, 2023, **17**(16), 16252–16263.
54 A. N. Colli, P. Peljo and H. H. Girault, High energy density MnO_4^-/MnO_4^{2-} redox couple for alkaline redox flow batteries, *Chem. Commun.*, 2016, **52**(97), 14039–14042.
55 M. Skyllas-Kazacos, M. Rychcik, R. G. Robins, A. G. Fane and M. A. Green, New all-vanadium redox flow cell, *J. Electrochem. Soc.*, 1986, **133**(5), 1057.
56 C. Xie, Y. Duan, W. Xu, H. Zhang and X. Li, A low-cost neutral zinc–iron flow battery with high energy density for stationary energy storage, *Angew. Chem., Int. Ed.*, 2017, **56**(47), 14953–14957.
57 Y. Long, Z. Xu, G. Wang, H. Xu, M. Yang, M. Ding, D. Yuan, C. Yan, Q. Sun, M. Liu and C. Jia, A neutral polysulfide/ferricyanide redox flow battery, *iScience*, 2021, **24**(10), 103157.
58 K. Lin, Q. Chen, M. R. Gerhardt, L. Tong, S. B. Kim, L. Eisenach, A. W. Valle, D. Hardee, R. G. Gordon, M. J. Aziz and M. P. Marshak, Alkaline quinone flow battery, *Science*, 2015, **349**(6255), 1529–1532.
59 T. Liu, X. Wei, Z. Nie, V. Sprenkle and W. Wang, A total organic aqueous redox flow battery employing a low cost and sustainable methyl viologen anolyte and 4-HO-TEMPO catholyte, *Adv. Energy Mater.*, 2016, **6**(3), 1501449.
60 B. Huskinson, M. P. Marshak, C. Suh, S. Er, M. R. Gerhardt, C. J. Galvin, X. Chen, A. Aspuru-Guzik, R. G. Gordon and M. J. Aziz, A metal-free organic–inorganic aqueous flow battery, *Nature*, 2014, **505**(7482), 195–198.

61 Y. K. Zeng, T. S. Zhao, X. L. Zhou, L. Wei and H. R. Jiang, A low-cost iron-cadmium redox flow battery for large-scale energy storage, *J. Power Sources*, 2016, **330**, 55–60.
62 K. B. Hatzell, M. Boota and Y. Gogotsi, Materials for suspension (semi-solid) electrodes for energy and water technologies, *Chem. Soc. Rev.*, 2015, **44**(23), 8664–8687.
63 Y. Lu and J. B. Goodenough, Rechargeable alkali-ion cathode-flow battery, *J. Mater. Chem.*, 2011, **21**(27), 10113–10117.
64 G. Schwartz, B. C. K. Tee, J. Mei, A. L. Appleton, D. H. Kim, H. Wang and Z. Bao, Flexible polymer transistors with high pressure sensitivity for application in electronic skin and health monitoring, *Nat. Commun.*, 2013, **4**(1), 1859.
65 F. Yang, S. M. A. Mousavie, T. K. Oh, T. Yang, Y. Lu, C. Farley, R. J. Bodnar, L. Niu, R. Qiao and Z. Li, Sodium–sulfur flow battery for low-cost electrical storage, *Adv. Energy Mater.*, 2018, **8**(11), 1701991.
66 Y. Wang, Y. Wang and H. Zhou, A Li–liquid cathode battery based on a hybrid electrolyte, *ChemSusChem*, 2011, **4**(8), 1087–1090.
67 B. Li and J. Liu, Progress and directions in low-cost redox-flow batteries for large-scale energy storage, *Natl. Sci. Rev.*, 2017, **4**(1), 91–105.
68 W. Zhang, Z. Wang, H. Wan, A.-M. Li, Y. Liu, S.-C. Liou, K. Zhang, Y. Ren, C. Jayawardana, B. L. Lucht and C. Wang, Revitalizing interphase in all-solid-state Li metal batteries by electrophile reduction, *Nat. Mater.*, 2025, **24**, 414–423.
69 R. M. Darling, K. G. Gallagher, J. A. Kowalski, S. Ha and F. R. Brushett, Pathways to low-cost electrochemical energy storage: A comparison of aqueous and nonaqueous flow batteries, *Energy Environ. Sci.*, 2014, **7**(11), 3459–3477.
70 T. Famprikis, P. Canepa, J. A. Dawson, M. S. Islam and C. Masquelier, Fundamentals of inorganic solid-state electrolytes for batteries, *Nat. Mater.*, 2019, **18**(12), 1278–1291.
71 C. Wang, J. T. Kim, C. Wang and X. Sun, Progress and prospects of inorganic solid-state electrolyte-based all-solid-state pouch cells, *Adv. Mater.*, 2023, **35**(19), 2209074.
72 M. Shao, Q. Chang, J.-P. Dodelet and R. Chenitz, Recent Advances in Electrocatalysts for Oxygen Reduction Reaction, *Chem. Rev.*, 2016, **116**(6), 3594–3657.
73 J. Zhang, W. Zhou, D. Zhao, Y.-C. Lu and D. Chao, Aqueous sulfur-based redox flow battery, *Nat. Rev. Electr. Eng.*, 2025, **2**, 215–217.
74 Z. Shi, Z. Tian, D. Guo, Y. Wang, Z. Bayhan, A. S. Alzahrani and H. N. Alshareef, Kinetically favorable Li–S battery electrolytes, *ACS Energy Lett.*, 2023, **8**(7), 3054–3080.
75 S. H. Ge, B. L. Yi and H. M. Zhang, Study of a high power density sodium polysulfide/bromine energy storage cell, *J. Appl. Electrochem.*, 2004, **34**(2), 181–185.
76 M. M. Gross and A. Manthiram, Aqueous polysulfide–air battery with a mediator-ion solid electrolyte and a copper sulfide catalyst for polysulfide redox, *ACS Appl. Energy Mater.*, 2018, **1**(12), 7230–7236.
77 M. Gao, S. Huang, F. Zhang, Y. M. Lee, S. Huang and Q. Wang, Successive ionic layer adsorption and reaction–deposited copper sulfide electrocatalyst for high-power polysulfide-based aqueous flow batteries, *Mater. Today Energy*, 2020, **18**, 100540.
78 C. Tan, J. Chen, X.-J. Wu and H. Zhang, Epitaxial growth of hybrid nanostructures, *Nat. Rev. Mater.*, 2018, **3**(2), 17089.
79 A. Pospischil, M. M. Furchi and T. Mueller, Solar-energy conversion and light emission in an atomic monolayer p–n diode, *Nat. Nanotechnol.*, 2014, **9**(4), 257–261.
80 D. Ma, B. Hu, W. Wu, X. Liu, J. Zai, C. Shu, T. Tadesse Tsega, L. Chen, X. Qian and T. L. Liu, Highly active nanostructured CoS_2/CoS heterojunction electrocatalysts for aqueous polysulfide/iodide redox flow batteries, *Nat. Commun.*, 2019, **10**(1), 3367.
81 Z. Wang, G. Lu, T. Wei, G. Meng, H. Cai, Y. Feng, K. Chu, J. Luo, G. Hu, D. Wang and X. Liu, Synergy of single atoms and sulfur vacancies for advanced polysulfide–iodide redox flow battery, *Nat. Commun.*, 2025, **16**(1), 2885.
82 L. Fan and I. I. Suni, Polysulfide reduction and oxidation at MoS_2, WS_2 and Cu-doped MoS_2 thin film electrodes, *J. Electrochem. Soc.*, 2019, **166**(8), A1471.
83 B. Chen, H. Huang, J. Lin, K. Zhu, L. Yang, X. Wang and J. Chen, Doping engineering of M-N-C electrocatalyst based membrane—electrode assembly for high-performance aqueous polysulfides redox flow batteries, *Adv. Sci.*, 2023, **10**(16), 2206949.
84 J. Lei, Y. Zhang, Y. Yao, Y. Shi, K. L. Leung, J. Fan and Y.-C. Lu, An active and durable molecular catalyst for aqueous polysulfide-based redox flow batteries, *Nat. Energy*, 2023, **8**(12), 1355–1364.
85 Z. Li and Y.-C. Lu, Polysulfide-based redox flow batteries with long life and low levelized cost enabled by charge-reinforced ion-selective membranes, *Nat. Energy*, 2021, **6**(5), 517–528.
86 Y. Xia, M. Ouyang, V. Yufit, R. Tan, A. Regoutz, A. Wang, W. Mao, B. Chakrabarti, A. Kavei, Q. Song, A. R. Kucernak and N. P. Brandon, A cost-effective alkaline polysulfide-air redox flow battery enabled by a dual-membrane cell architecture, *Nat. Commun.*, 2022, **13**(1), 2388.
87 M. M. Gross and A. Manthiram, Long-life polysulfide–polyhalide batteries with a mediator-ion solid electrolyte, *ACS Appl. Energy Mater.*, 2019, **2**(5), 3445–3451.
88 S. Sreenath, P. S. Nayanthara, C. M. Pawar, A. Ash, B. Bhatt, V. Verma and R. K. Nagarale, An aqueous polysulfide redox flow battery with a semi-fluorinated cation exchange membrane, *Energy Adv.*, 2024, **3**(1), 203–214.